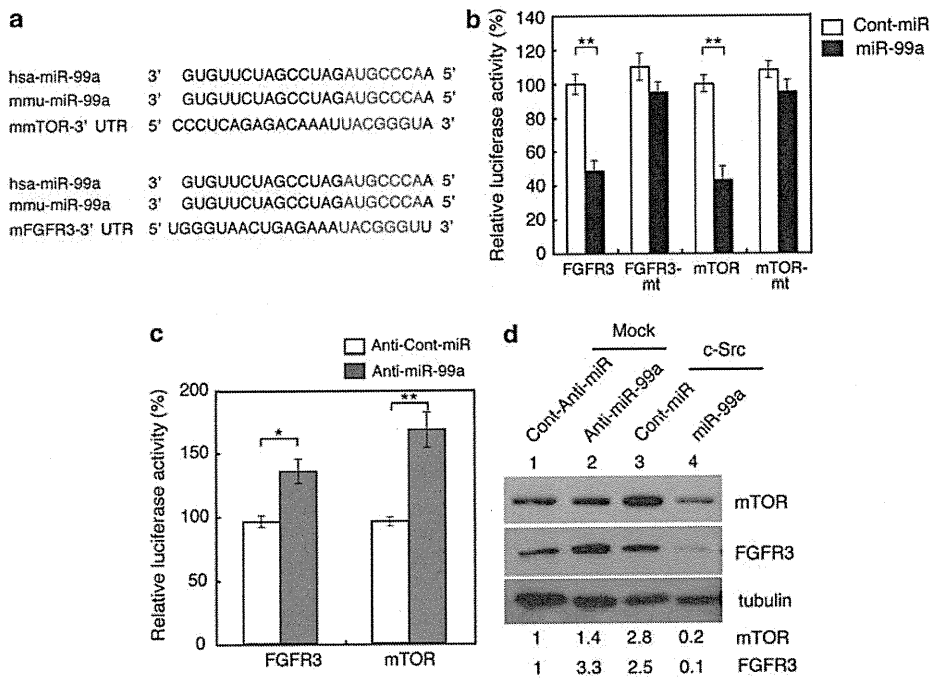

Figure 3 miR-99a targets mTOR and FGFR3. (**a**) Alignment of RNA sequences of human and mouse miR-99a and the potential miR-99a binding sequences in the mTOR and FGFR3 3′-untranslated regions. The seed sequence of miR-99a and its binding sequences are shown in red. (**b**) pMIR-mTOR and pMIR-FGFR3 luciferase reporter constructs, containing either wild-type or mutated (mt) mTOR and FGFR3 3′-untranslated regions, were transfected into c-Src-transformed cells. Relative *Renilla* luciferase expression was standardized to a transfection control. Relative values ± s.d. were obtained from three independent assays. (**c**) $Csk^{-/-}$ cells treated with anti-cont-miR or anti-miR-99a were transfected with pMIR-mTOR and pMIR-FGFR3 constructs, and the relative luciferase activity was determined. Relative values ± s.d. were obtained from three independent assays. (**d**) $Csk^{-/-}$ cells (Mock) were transfected with the control or anti-miR-99a, and c-Src-transformed cells (c-Src) were transfected with the control or miR-99a. Total cell lysates were immunoblotted with the indicated antibodies. The relative expression levels of mTOR or FGFR3 are shown at the bottom of the panels. $*P<0.05$ and $**P<0.01$, by Student's *t*-test.

the expression of miR-99a (lanes 3 vs 4). In contrast, inactivation of miR-99a by anti-miR-99a increased mTOR and FGFR3 expressions (lanes 1 vs 2). These findings show that miR-99a can target endogenous mTOR/FGFR3, and suggest that downregulation of miR-99a by c-Src activation is tightly associated with the upregulation of mTOR/FGFR3 in c-Src-transformed cells.

Roles of mTOR and FGFR3 in c-Src-mediated tumor growth

To examine the role of upregulation of mTOR and FGFR3 in c-Src-transformed cells, we performed rescue experiments using open-reading frames (ORFs) of mTOR and FGFR3 cDNAs. The expression of miR-99a in c-Src-transformed cells reduced mTOR protein levels as well as the activity of p70S6K, a critical downstream effector of mTOR (Figure 4a, lane 2). When the mTOR ORF was introduced into miR-99a-treated cells, mTOR protein and the activity of p70S6K were significantly increased (Figure 4a, lane 4). Although the extent of these upregulations was not so remarkable, it was sufficient to restore a significant colony-forming activity in these cells (Figure 4b). We also observed that inhibition of mTOR activity with the selective inhibitor rapamycin effectively suppressed tumor growth of c-Src-transformed cells as well as A549 cells that have c-Src upregulation (Supplementary Figure 2). These findings suggest that the mTOR activity is correlated with the ability of c-Src to induce tumor growth.

To further verify the significance of upregulation of mTOR protein levels in tumor growth, we differentially overexpressed mTOR protein in non-transformed $Csk^{-/-}$ cells, in which c-Src is activated insufficiently for cell transformation (Oneyama *et al.*, 2008). The expression of mTOR protein dose-dependently enhanced p70S6K activity and the colony-forming activity of these cells, and the expression of mTOR at nearly twice the normal level was sufficient to induce colony formation (Figure 4c). More interestingly, when mTOR was upregulated by inactivating miR-99a using anti-miR-99a, non-transformed $Csk^{-/-}$ cells gained the ability to form colonies in a manner dependent on the concentrations of anti-miR-99a (Figure 4d and Supplementary Figure 3). These results suggest that mTOR can dose-dependently control the potential for tumor growth, within a range regulatable by miR-99a. However, the colony-forming activity of mTOR-overexpressing cells (Figure 4c, lane 3) was significantly weaker than that of c-Src-transformed cells (Figure 4c, lane 4

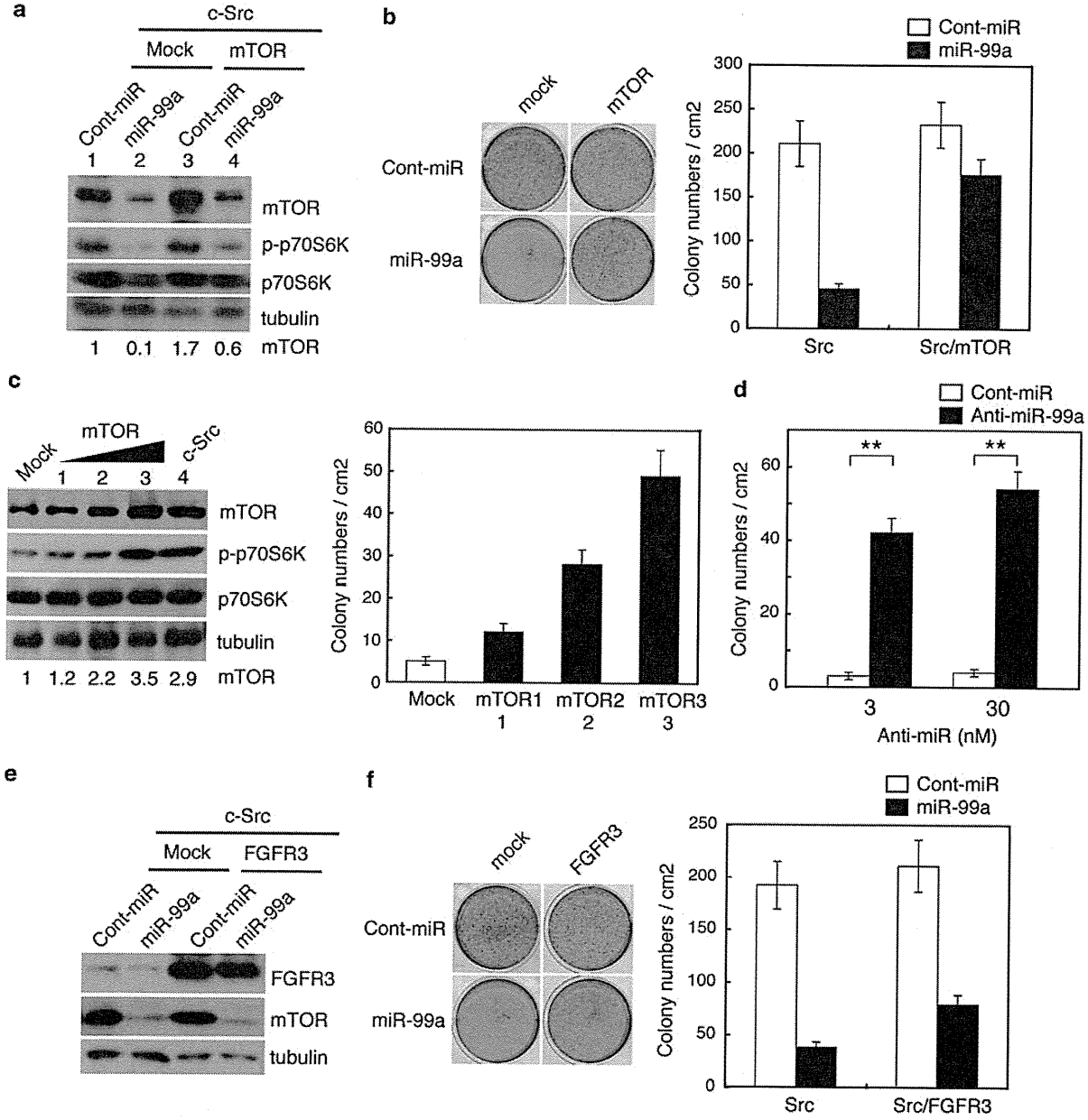

Figure 4 Roles of mTOR and FGFR3 in c-Src-mediated tumor growth. (**a**) c-Src-transformed cells transfected with the mTOR ORF cDNA were treated with cont-miR or miR-99a, and the total cell lysates were immunoblotted with the indicated antibodies. The relative expression levels of mTOR are shown at the bottom of the panels. (**b**) Soft-agar colony formation assays for cells used in (**a**). Representative dishes from three independent experiments are shown (left panels). The mean number of colonies ± s.d. was obtained from three independent experiments (right panel). (**c**) Total cell lysates of $Csk^{-/-}$ cells expressing different amounts of mTOR were immunoblotted with the indicated antibodies (left panels). The relative expression levels of mTOR are shown at the bottom of the panels. The cells were subjected to soft-agar colony formation assays (right panel). The mean number of colonies ± s.d. was obtained from three independent experiments (right panel). (**d**) Soft-agar colony formation assays of $Csk^{-/-}$ cells treated with indicated concentrations of anti-miR-99a or anti-cont-miR. The mean number of colonies ± s.d. was obtained from three independent experiments. $^{**}P<0.01$, by Student's *t*-test. (**e**) c-Src-transformed cells transfected with the FGFR3 ORF cDNA were treated with cont-miR or miR-99a, and the total cell lysates were immunoblotted with the indicated antibodies. (**f**) Soft-agar colony formation assays for cells used in (**e**). The mean number of colonies ± s.d. was obtained from three independent experiments (right panel).

and Figure 2c). This indicates that mTOR is required, but insufficient for inducing full transformation, because critical pathways, such as the MAPK pathway, which are required for cell proliferation, were not activated by the expression of mTOR.

On the other hand, the transfection of c-Src-transformed cells with the FGFR3 ORF induced a substantial overexpression of FGFR3 protein even in miR-99a-treated cells (Figure 4e), but it only moderately rescued c-Src-mediated tumor growth (Figure 4f).

However, it should be noted that mTOR was also downregulated by miR-99a even in FGFR3-overexpressing cells. Thus, it seems probable that the recovery of tumor growth by FGFR3 expression may be cancelled by the downregulation of mTOR. In contrast, the selective FGFR3 inhibitor PD173074 (Trudel *et al.*, 2004) was able to dose-dependently suppress colony-forming activity of c-Src-transformed cells and A549 cells (Supplementary Figure 4). Therefore, it is likely that upregulation of FGFR3 can also contribute to c-Src-mediated tumor growth by acting upstream of mTOR.

miR-99a is downregulated by Src-related oncogenic pathways

To follow the signaling pathway leading to the downregulation of miR-99a, we first tested the contribution of epidermal growth factor receptor (EGFR) signaling involving c-Src activation. When murine embryonic fibroblasts (MEFs) were stimulated with EGF, the kinase activity of c-Src was increased by auto-phosphorylation at Y418 (Figure 5a, left panels), and the cells showed morphological transformation (data not shown). In these EGF-transformed cells, the expression of miR-99a was appreciably downregulated (Figure 5b). Conversely, the expression of mTOR and FGFR3 was upregulated by EGF stimulation (Figure 5a, right panels). These results indicate that the expression of miR-99a can also be regulated downstream of EGFR signaling. To further identify the pathway downstream of this EGFR signaling, we examined the effect of an MAPK/ERK kinase (MEK) inhibitor (U0126) or a PI3K inhibitor (LY294002) on EGF-induced downregulation of miR-99a. The expression of miR-99a was significantly restored by treatment with U0126, but not by LY294002 (Figure 5c), suggesting that miR-99a expression is mainly regulated via the MEK/ERK pathway.

These findings led to the question as to whether the downregulation of miR-99a can be induced by other oncogenes such as v-Src, H-RasV12 and K-RasG12, all of which can activate the MEK/ERK pathway. As expected, transformation by these oncogenes induced a significant downregulation of miR-99a to a level similar to that observed in c-Src-transformed cells (Figures 5d and 1b), and inversely caused upregulation of mTOR and FGFR3 proteins (Figure 5e). The ectopic expression of miR-99a in these cells downregulated mTOR and FGFR3 proteins (Figure 5e) and significantly suppressed their colony-forming activities (Figure 5f). These findings suggest that the expression of miR-99a can be downregulated via the Ras-MEK/ERK pathway downstream of activated EGFR/Src.

miR-99a in human cancer cells

To examine if the miR-99a–mTOR/FGFR3 axis is indeed functional in human cancers, we determined the expression levels of miR-99a and mTOR/FGFR3 in several human lung cancer cell lines. Western blot analysis showed a significant upregulation of mTOR and FGFR3 in all of the lung cancer cell lines examined (Figure 6a). In contrast, qRT–PCR analysis revealed that the expression of miR-99a was greatly reduced in most of the lung cancer cells (Figure 6b). The levels of mTOR and FGFR3 were not necessarily correlated with the amount of protein or the activity status of c-Src (pY418), which reflects the potential contribution of other signaling components to human cancers (Figure 6a). Human cancer cells contain multiple mutations in oncogenes and tumor suppressor genes. A549 has c-Src upregulation and a *K-Ras* mutation; Lu99 harbors a *K-Ras* mutation; H69 and H526 have an *N-myc* amplification; PC9 has an *EGFR* mutation; and PC10 has a c-Src upregulation as well as a *PTEN* mutation (Yokota and Kohno, 2004; Noro *et al.*, 2006). These lines of information suggest that there is an upregulation of the Src-related oncogenic pathways in these cells, which may account for the downregulation of miR-99a observed in various human cancer cells.

To examine the functional link between miR-99a and mTOR/FGFR3 in human cancers, we ectopically expressed miR-99a in lung (A549, PC10 and Lu99) cancer cells. The expression of miR-99a in A549 cells induced a significant downregulation of mTOR and FGFR3 proteins (Figure 6c) and significantly suppressed the colony-forming activity of A549, PC10 and Lu99 cells (Figure 6d). Conversely, knockdown of miR-99a in A549 cells increased mTOR and FGFR3 expressions and colony-forming activity (Figures 6c and e). In addition, inactivation of miR-99a induced an anchorage-independent growth in human normal epithelial cells such as HEK293 and HaCaT (Supplementary Figure S5). These results suggest that miR-99a downregulation is involved in carcinogenesis and malignancy in human cells.

The importance of mTOR upregulation in tumor growth was further confirmed by observing that short hairpin RNA-mediated mTOR knockdown in A549 cells appreciably suppressed colony-forming activity (Supplementary Figure S6). Interestingly, the effect of miR-99a expression was more evident *in vivo*: tumorigenesis in nude mice was potently suppressed by miR-99a expression in A549 cells (Figure 6f). These findings suggest that miR-99a is involved in regulating tumor growth of a subset of human cancer cells by targeting mTOR/FGFR3.

miR-99a in human cancer tissues

Finally, we verified the role of miR-99a in human cancers by determining miR-99a expression in lung primary tumors as well as in adjacent normal tissues using qRT–PCR. In most of the tumor samples examined, miR-99a was significantly downregulated (Figure 7a). Immunohistochemical analysis of mTOR and FGFR3 expression in lung tumor specimens showed that mTOR and FGFR3 immunoreactivity was greatly increased in all of the five primary tumor regions in comparison to the adjacent normal tissues (Figure 7b). These observations suggest that there is an inverse correlation between the expressions of miR-99a and mTOR/FGFR3 even in human cancer tissues.

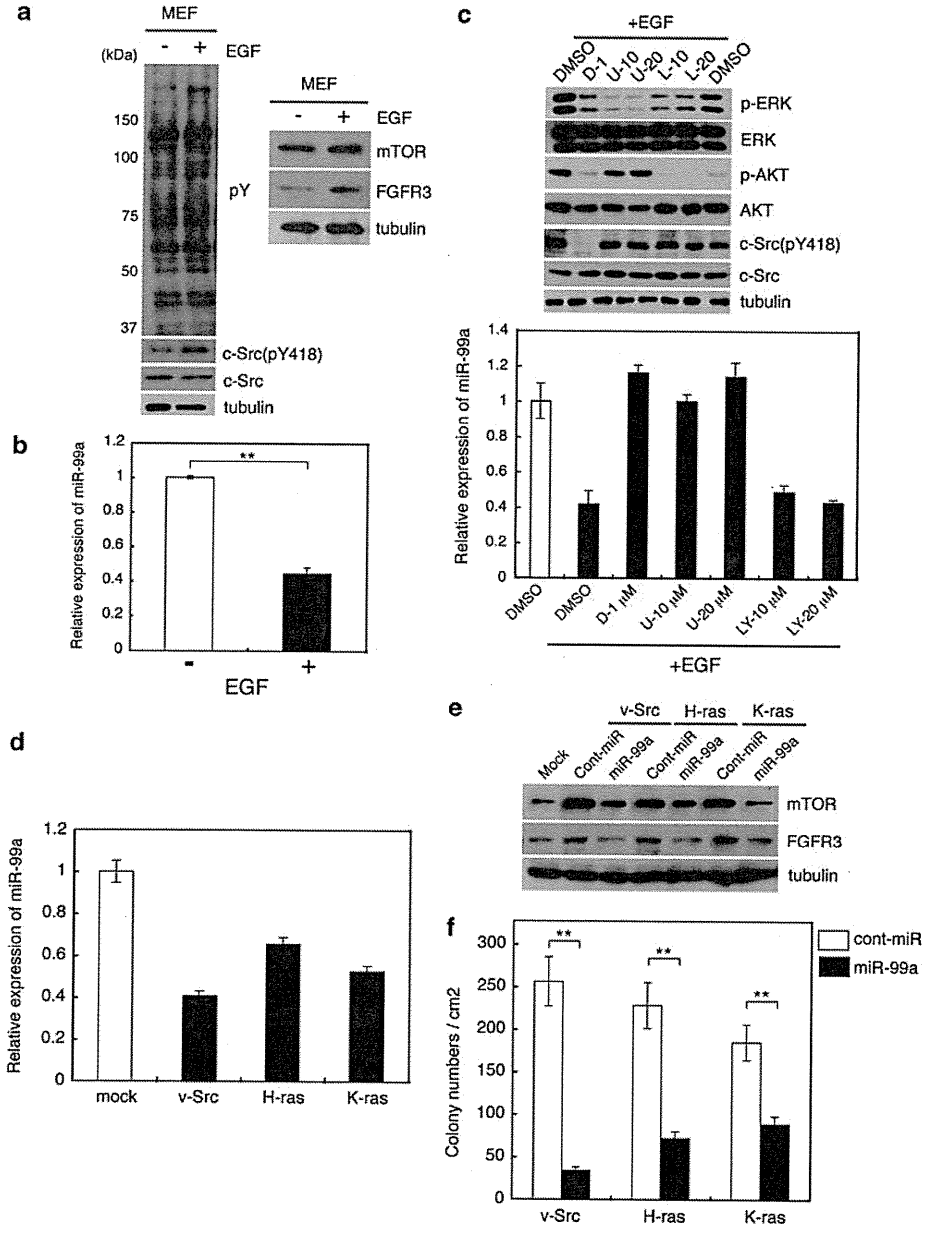

Figure 5 miR-99a is downregulated in cells transformed by other oncogenic signals. (**a**) Total cell lysates from MEFs were stimulated with or without 10 ng/ml EGF for 4 days and immunoblotted with the antibodies indicated. (**b**) miR-99a expression levels were assessed by qRT–PCR in MEFs stimulated with (black) or without (white) EGF. (**c**) MEFs were treated with or without Dasatinib (D), U0126 (U) or LY294002 (L) at the indicated concentrations in the presence of EGF for 2 days, and the total cell lysates were immunoblotted with the antibodies indicated (upper panels). The expression levels of miR-99a were assessed by qRT–PCR (lower panel). (**d**) The expression levels of miR-99a in MEFs transformed by v-Src, H-RasV12 or K-RasG12 were assessed by qRT–PCR. Relative values ± s.d. were obtained from three independent assays (**b–d**). (**e**) MEFs transformed by v-Src, H-RasV12 or K-RasG12 were treated with cont-miR or miR-99a, and the total cell lysates were immunoblotted with the antibodies indicated. (**f**) MEFs analyzed in (**e**) were subjected to soft-agar colony formation assay. The mean number of colonies ± s.d. was obtained from three independent experiments. $^{**}P<0.01$, by Student's *t*-test.

Overall, the present findings suggest that downregulation of miR-99a is induced by the activation of Src-related oncogenic pathways in various human cancers, and is tightly associated with the promotion of tumor growth via upregulation of mTOR/FGFR3 pathways (Figure 7c).

Discussion

To elucidate the molecular mechanisms underlying c-Src-mediated transformation, we previously established an experimental system using Csk-deficient cells (Oneyama *et al.*, 2008). In this study, we used this

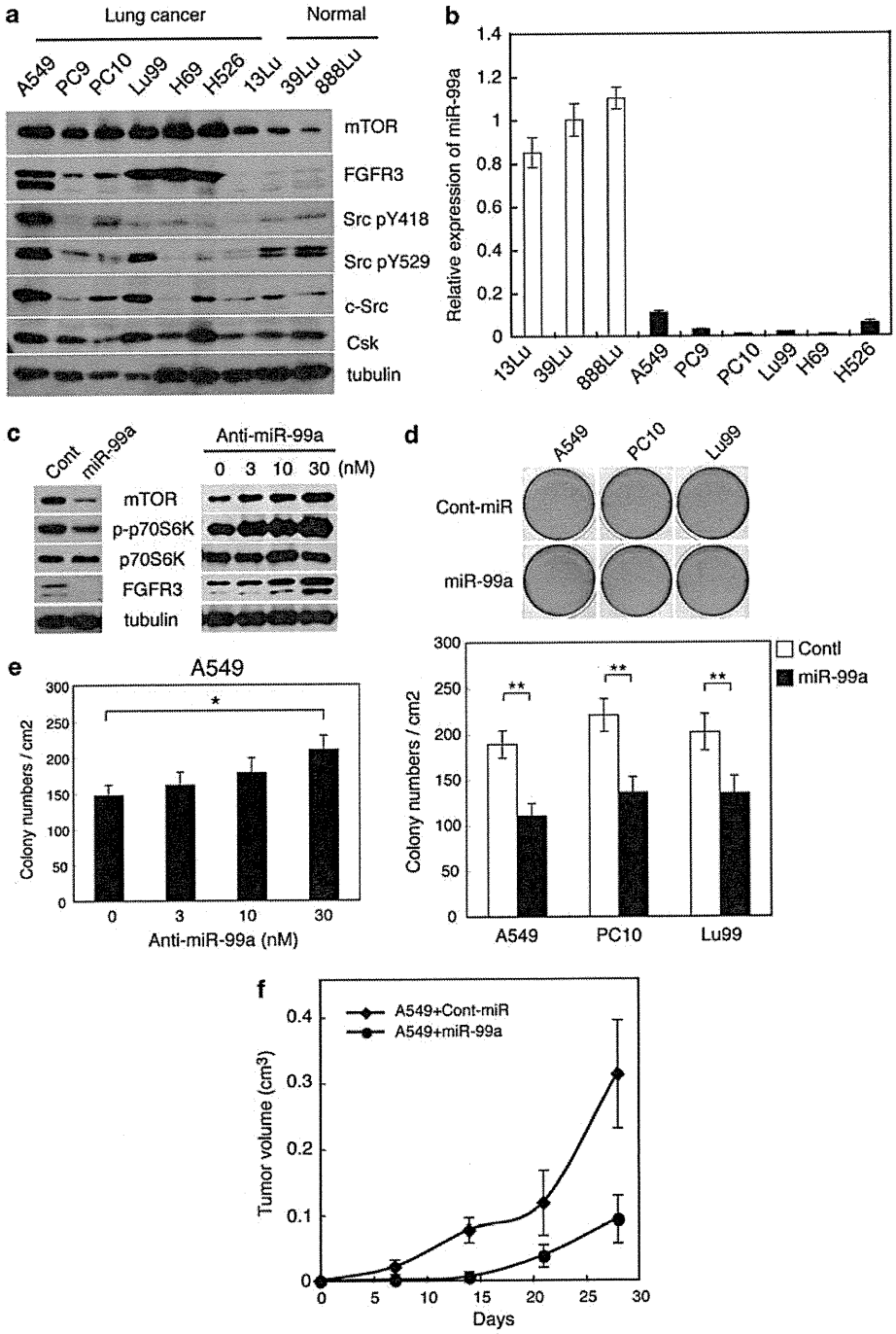

Figure 6 miR-99a in human lung cancer cells. (**a**) Total cell lysates from the indicated lung cancer cell lines were immunoblotted with the indicated antibodies. (**b**) The expression levels of miR-99a in these cells were assessed by qRT–PCR. The mean values ± s.d. were obtained from three independent experiments. (**c**) A549 cells were transfected with miR-99a or anti-miR-99a, followed by immunoblotting with the indicated antibodies. (**d**) A549, PC10 and Lu99 cells were treated with miR-99a or control-miR were subjected to the soft-agar colony formation assay. Representative dishes from three independent experiments are shown (upper panels). The mean number of colonies ± s.d. was obtained from three independent experiments in each case (lower panel). (**e**) Soft-agar colony formation assays of A549 cells treated with indicated concentrations of anti-miR-99a. The mean number of colonies ± s.d. was obtained from three independent experiments. (**f**) A549 cells transfected with or without miR-99a were inoculated subcutaneously into nude mice. Means ± s.d. of tumor volume (cm^3) obtained from three mice are plotted vs time after inoculation (days). $*P<0.05$ and $**P<0.01$, by Student's *t*-test.

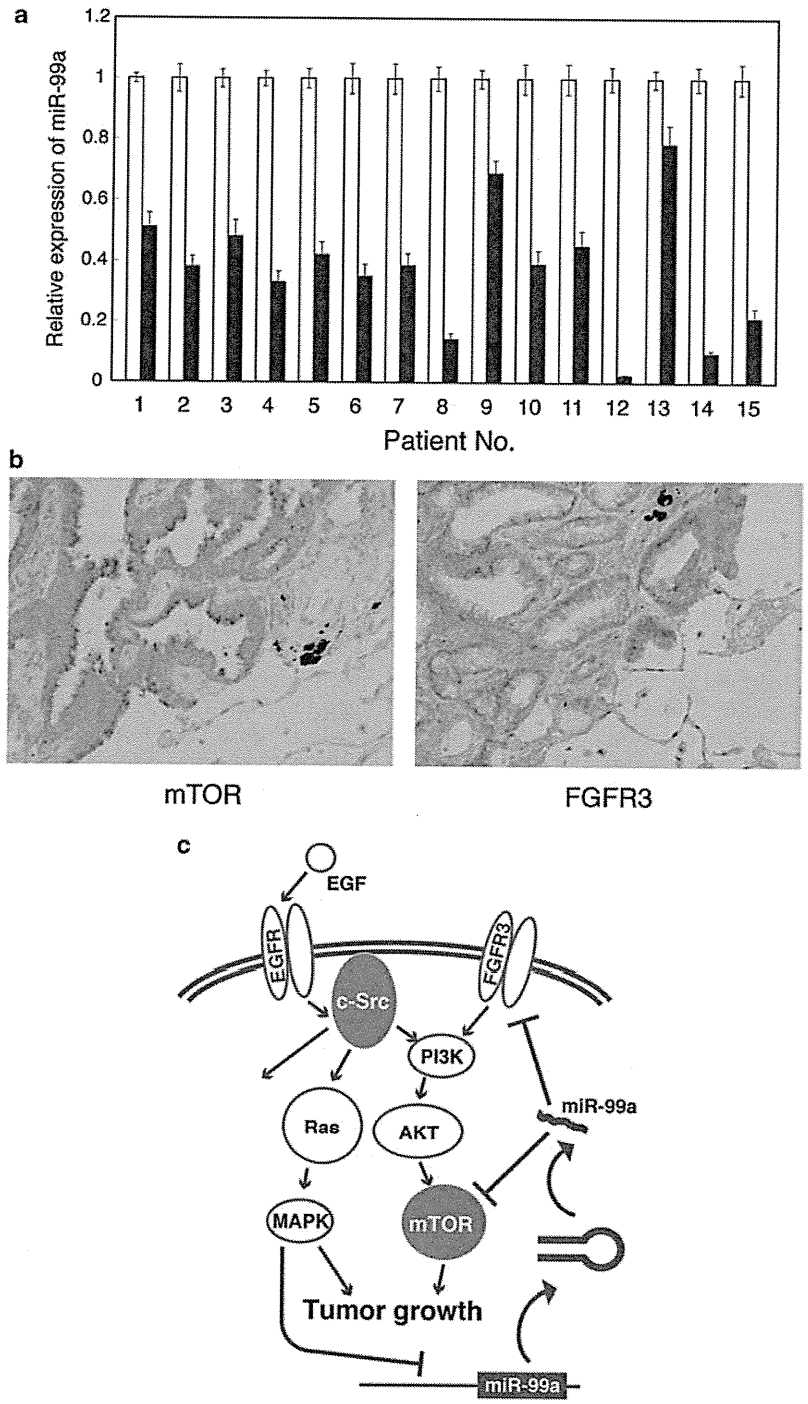

Figure 7 miR-99a in lung cancer tissues. (**a**) The expression of miR-99a in human lung tumors (black) and the corresponding normal tissue (white) from individual patients (1–15) was analyzed by qRT–PCR. Relative values ± s.d. were obtained from three independent assays. (**b**) Immunohistochemistry for mTOR and FGFR3 in lung adenocarcinoma and normal lung tissue samples (×400). Representative images from five samples are shown. (**c**) A schematic model of the function of miR-99a. The downregulation of miR-99a mediated by the Src-related oncogenic pathway results in the upregulation of mTOR and FGFR3, which in turn activates protein synthesis and the PI3K pathway, respectively, leading to the promotion of cell growth and survival.

system to study the potential role of miRNAs in c-Src-mediated tumor growth. The miRNA profiling identified seven miRNAs that were downregulated by c-Src transformation. A previous study showed that the expression of nine of 95 miRNAs that had been implicated in cancer, development and apoptosis was

affected by v-Src transformation (Li *et al.*, 2009). More recently, it was shown that 29 miRNAs were differentially expressed during transformation of MCF10A-ER-Src cells (Iliopoulos *et al.*, 2010). However, the miRNA species identified in the previous studies, such as miR-126, -218, -224, -21 or -181b-1 relevant to Src signaling and cancer, are not necessarily consistent with those identified in this study. Although the actual reasons are currently unclear, this inconsistency might be due to the difference in the pathways activated by v-Src and c-Src, or related to the cellular context. Because upregulation of c-Src protein and/or activity, rather than gain-of-function mutations in the *c-src* gene, widely contributes to the progression of human cancers, c-Src-transformed cells were used to identify miRNAs crucial for regulating human cancers.

Of the miRNAs downregulated by c-Src activation, we first focused on miR-99a, because recent reports suggested a potential tumor suppressor function of this miRNA in various human cancers (Yamada *et al.*, 2008; Doghman *et al.*, 2010; Gao *et al.*, 2010). We showed that it targets mTOR and FGFR3, both of which have been implicated in human cancers (Eswarakumar *et al.*, 2005; Guertin and Sabatini, 2007). A more recent study also showed that miR-99a can target the IGF-IR-mTOR-raptor pathway in a specific subset of human cancers (Doghman *et al.*, 2010), suggesting a role for miR-99a in regulating the oncogenic function of mTOR. However, the functional link between miR-99a and cancer progression is unclear, and the mechanisms underlying the downregulation of miR-99a in cancers remains to be addressed. This study provides the first firm evidence for tumor suppressive role of miR-99a and suggests that the expression of miR-99a is regulated via the Src-related oncogenic pathways involving EGFR, c-Src, K/H-Ras and MEK/ERK. In addition, the first evidence that perturbation of mTOR protein levels can directly contribute to controlling tumor growth is presented. As the Src-related oncogenic pathway is frequently activated in various human cancers, the functional analysis of the miR-99a–mTOR/FGFR3 axis driven by the EGFR/Src/Ras/MAPK pathway represents a great leap forward in our understanding of cancer etiology. Indeed, various human cancer cells, which harbor deregulation of c-Src, EGFR, K-Ras or N-myc, were shown to exhibit downregulation of miR-99a and upregulation of mTOR/FGFR3. The inhibition of mTOR function or introduction of miR-99a successfully suppressed tumor growth in certain types of human cancer cells. Furthermore, the existence of an inverse correlation between miR-99a and mTOR/FGFR3 in primary human cancer tissues was shown. Considering the crucial role of mTOR in various cancers, these observations support our proposal that the Src pathway–miR-99a–mTOR/FGFR3 axis is important in controlling tumor growth in a wide array of human cancers.

The substantial downregulation of miR-99a in human lung tumors suggests a crucial role for miR-99a as a regulator of these cancers. The *miR-99a* gene is located on chromosome 21q21.1, which was identified as a minimal region where loss of heterozygosity frequently occurs in cases of human lung cancer (Yamada *et al.*, 2008). The qRT–PCR analysis of miR-99a expression levels in a panel of lung cancer cell lines revealed a substantial reduction of miR-99a expression to less than one-tenth that of normal lung expression. To examine the possibility that these cell lines carry a homozygous deletion at 21q21.1, loss of heterozygosity analysis of A549 and PC10 cells was performed by genomic PCR, which confirmed that the 21q21.1 region is intact in these cells (data not shown). This observation suggests that activation of the Src/Ras-related oncogenic pathway, for example, *K-Ras* mutation, more widely contributes to the downregulation of miR-99a in cancer cells. However, downstream mechanisms that lead to changes in *miR-99a* gene expression remain unclear. Further extensive analysis will be necessary to elucidate the precise mechanism of miR-99a downregulation.

We also observed that ectopic expression of miR-99a suppressed anchorage-independent growth and tumorigenesis of c-Src-transformed cells, but it only moderately affected cell morphology. This could be attributed to the specific roles of mTOR and FGFR3 in regulating tumor growth and survival, respectively. On the basis of these findings, we propose a hypothetical model for the function of the miR-99a–mTOR/FGFR3 axis in tumor growth (Figure 7c). Downregulation of miR-99a caused by the activation of Src-related pathways results in the upregulation of mTOR and FGFR3, which in turn activate protein synthesis and the PI3K pathway, respectively, and promote tumor growth and survival. Earlier studies suggested that Src activity plays a critical role in the deregulation of mTOR signaling pathways, but the functional link between Src and mTOR was unclear (Penuel and Martin, 1999; Vojtechova *et al.*, 2008). It was also seen that mTOR is often overexpressed and activated in a wide variety of human cancers (Hay, 2005; Sabatini, 2006; Nozawa *et al.*, 2007); however, the underlying mechanisms remained unknown. This model for miR-99a function would provide a missing link between Src, mTOR and cancer progression.

The potential role of miRNA in mTOR regulation has previously been shown in studies of miR-100, an miRNA that contains the same seed sequences as miR-99a. It has been reported that miR-100 is downregulated in human cytomegalovirus infection and that re-expression of miR-100 reduces mTOR protein levels (Wang *et al.*, 2008). In addition, miR-100 is downregulated in clear cell ovarian cancer (Nagaraja *et al.*, 2010) and childhood adrenocortical tumors (Doghman *et al.*, 2010), and the overexpression of miR-100 inhibits mTOR signaling and enhances sensitivity to a mTOR inhibitor RAD001 (Nagaraja *et al.*, 2010). More recently, miR-199a-3p was also shown to be downregulated and target mTOR in hepatocarcinoma cells (Fornari *et al.*, 2010). These features of miR-100 and miR-199a-3p are quite similar to those of miR-99a, suggesting that mTOR expression might be regulated redundantly by these closely related miRNAs. However, downregulation of miR-100 and miR-199a-3p in c-Src-

transformed cells could not be detected (data not shown); this indicates that the expression of miR-100 and miR-199a-3p may be regulated through a pathway independent of the Src-related pathway or in different cellular contexts. Nonetheless, these findings strongly highlight a critical role of miRNA-mediated regulation of mTOR signaling in controlling tumor growth in various human cancers.

In conclusion, we have shown a crucial role for the Src–miR-99a–mTOR/FGFR3 axis in controlling tumor growth. Our study provides insights into the function of this new signaling axis, and offers new opportunities for therapeutic intervention in a wide array of human cancers.

Materials and methods

Pre-miR-99a and anti-miR-99a transfection
miR-99a precursor (PM10719), antisense miR-99a (AM11465) and control miR (AM17110) were purchased from Applied Biosystems (Foster City, CA, USA). The day before transfection, 2.5×10^5 cells were seeded onto six-well plates. Different concentrations of precursors (0.3–30 nM) and inhibitors (3–30 nM), as well as the negative control, were transfected using Lipofectamine RNAiMAX in 16 µl per six-well plates according to the manufacturer's instructions (Invitrogen, Carlsbad, CA, USA). Using this approach, 90% of cells were transfected as judged by comparison to FAM-labeled controls (AM17121; Applied Biosystems).

Soft-Agar colony formation assay
Single-cell suspensions of 2×10^4 cells were plated in six-well culture dishes in 1.5 ml of Dulbecco's modified Eagle's medium containing 10% fetal calf serum and 0.36% agar on a layer of 2.5 ml of the same medium containing 0.7% agar. Colonies were stained with 3-(4,5-dimethylthiazol-2-yl)- 2,5-diphenyltetrazolium bromide (Sigma, St Louis, MO, USA) 7–14 days after plating, and micrographs of the stained colonies were used to count the numbers of colonies.

Tumorigenesis assays
Immunodeficient mice (BALB/c AJcl-nu/nu; Japan CLEA, Tokyo, Japan) were injected subcutaneously with 1×10^6 cells suspended in 200 µl of serum-free Dulbecco's modified Eagle's medium at one location. Tumors were monitored every 2 or 3 days and the tumor volume was estimated using the following formula: $0.5 \times L \times W^2$. At least three mice were used in each experiment. The mice used for this study were handled in strict adherence with local governmental and institutional animal care regulations.

Immunohistochemistry
Histological specimens were fixed in 10% formalin and routinely processed for paraffin embedding. Histological sections 4-µm thick were stained with hematoxylin and eosin and reviewed by two pathologists (JI and EM) to define the cancerous and corresponding normal tissues. An immunoperoxidase procedure was performed on the paraffin-embedded sections as described below. After antigen retrieval using a Pascal pressurized heating chamber (Dako A/S, Glostrup, Denmark), the sections were incubated with anti-mTOR or anti-FGFR3 antibody that was diluted at 1:50. Cells were then treated with a ChemMate EnVision kit (Dako). Diaminobenzidine (Dako) was used as a chromogen. As a negative control, staining was carried out in the absence of primary antibody. Stained sections were evaluated independently by two pathologists (JI and EM).

Conflict of interest

The authors declare no conflicts of interest.

Acknowledgements

We thank Drs A Imamoto, T Akagi and M Yutsudo for generous gifts of reagents. This work was supported by a Grant-in-aid for Young Scientists from the Ministry of Education, Culture, Sports, Science and Technology of Japan and The Exciting Leading-Edge Research Project at Osaka University.

References

Ambros V. (2004). The functions of animal microRNAs. *Nature* **431**: 350–355.
Bartel DP. (2004). MicroRNAs: genomics, biogenesis, mechanism, and function. *Cell* **116**: 281–297.
Bartel DP. (2009). MicroRNAs: target recognition and regulatory functions. *Cell* **136**: 215–233.
Brown M, Cooper J. (1996). Regulation, substrates and functions of src. *Biochim Biophys Acta* **1287**: 121–149.
Calin GA, Croce CM. (2006). MicroRNA signatures in human cancers. *Nat Rev Cancer* **6**: 857–866.
Catto JW, Miah S, Owen HC, Bryant H, Myers K, Dudziec E *et al.* (2009). Distinct microRNA alterations characterize high- and low-grade bladder cancer. *Cancer Res* **69**: 8472–8481.
Doghman M, El Wakil A, Cardinaud B, Thomas E, Wang J, Zhao W *et al.* (2010). Regulation of insulin-like growth factor-mammalian target of rapamycin signaling by microRNA in childhood adrenocortical tumors. *Cancer Res* **70**: 4666–4675.
Engelman JA. (2009). Targeting PI3K signalling in cancer: opportunities, challenges and limitations. *Nat Rev Cancer* **9**: 550–562.
Esquela-Kerscher A, Slack FJ. (2006). Oncomirs—microRNAs with a role in cancer. *Nat Rev Cancer* **6**: 259–269.
Eswarakumar VP, Lax I, Schlessinger J. (2005). Cellular signaling by fibroblast growth factor receptors. *Cytokine Growth Factor Rev* **16**: 139–149.
Fornari F, Milazzo M, Chieco P, Negrini M, Calin GA, Grazi GL *et al.* (2010). MiR-199a-3p regulates mTOR and c-Met to influence the doxorubicin sensitivity of human hepatocarcinoma cells. *Cancer Res* **70**: 5184–5193.
Frame M. (2002). Src in cancer: deregulation and consequences for cell behaviour. *Biochim Biophys Acta* **1602**: 114–130.
Gao W, Shen H, Liu L, Xu J, Shu Y. (2010). MiR-21 overexpression in human primary squamous cell lung carcinoma is associated with poor patient prognosis. *J Cancer Res Clin Oncol* (e-pub ahead of print 17 February 2011; DOI:10.1007/s00432-011-0976-2).
Guertin DA, Sabatini DM. (2007). Defining the role of mTOR in cancer. *Cancer Cell* **12**: 9–22.
Hakak Y, Martin GS. (1999). Ubiquitin-dependent degradation of active Src. *Curr Biol* **9**: 1039–1042.
Hay N. (2005). The Akt-mTOR tango and its relevance to cancer. *Cancer Cell* **8**: 179–183.
Hay N, Sonenberg N. (2004). Upstream and downstream of mTOR. *Genes Dev* **18**: 1926–1945.
He L, Hannon GJ. (2004). MicroRNAs: small RNAs with a big role in gene regulation. *Nat Rev* **5**: 522–531.

Iliopoulos D, Jaeger SA, Hirsch HA, Bulyk ML, Struhl K. (2010). STAT3 activation of miR-21 and miR-181b-1 via PTEN and CYLD are part of the epigenetic switch linking inflammation to cancer. *Mol Cell* **39**: 493–506.

Ingley E. (2008). Src family kinases: regulation of their activities, levels and identification of new pathways. *Biochim Biophys Acta* **1784**: 56–65.

Irby R, Mao W, Coppola D, Kang J, Loubeau J, Trudeau W *et al.* (1999). Activating SRC mutation in a subset of advanced human colon cancers. *Nat Genet* **21**: 187–190.

Irby R, Yeatman T. (2000). Role of Src expression and activation in human cancer. *Oncogene* **19**: 5636–5642.

Ishizawar R, Parsons S. (2004). c-Src and cooperating partners in human cancer. *Cancer Cell* **6**: 209–214.

Li X, Shen Y, Ichikawa H, Antes T, Goldberg GS. (2009). Regulation of miRNA expression by Src and contact normalization: effects on nonanchored cell growth and migration. *Oncogene* **28**: 4272–4283.

Liu P, Cheng H, Roberts TM, Zhao JJ. (2009). Targeting the phosphoinositide 3-kinase pathway in cancer. *Nat Rev Drug Discov* **8**: 627–644.

Menon S, Manning BD. (2008). Common corruption of the mTOR signaling network in human tumors. *Oncogene* **27**(Suppl 2): S43–S51.

Nada S, Okada M, MacAuley A, Cooper JA, Nakagawa H. (1991). Cloning of a complementary DNA for a protein-tyrosine kinase that specifically phosphorylates a negative regulatory site of p60c-src. *Nature* **351**: 69–72.

Nagaraja AK, Creighton CJ, Yu Z, Zhu H, Gunaratne PH, Reid JG *et al.* (2010). A link between mir-100 and FRAP1/mTOR in clear cell ovarian cancer. *Mol Endocrinol* **24**: 447–463.

Nagayama K, Kohno T, Sato M, Arai Y, Minna JD, Yokota J. (2007). Homozygous deletion scanning of the lung cancer genome at a 100-kb resolution. *Genes Chromosomes Cancer* **46**: 1000–1010.

Nam EJ, Yoon H, Kim SW, Kim H, Kim YT, Kim JH *et al.* (2008). MicroRNA expression profiles in serous ovarian carcinoma. *Clin Cancer Res* **14**: 2690–2695.

Noro R, Gemma A, Kosaihira S, Kokubo Y, Chen M, Seike M *et al.* (2006). Gefitinib (IRESSA) sensitive lung cancer cell lines show phosphorylation of Akt without ligand stimulation. *BMC Cancer* **6**: 277.

Nozawa H, Watanabe T, Nagawa H. (2007). Phosphorylation of ribosomal p70 S6 kinase and rapamycin sensitivity in human colorectal cancer. *Cancer Lett* **251**: 105–113.

Okada M, Nada S, Yamanashi Y, Yamamoto T, Nakagawa H. (1991). CSK: a protein-tyrosine kinase involved in regulation of src family kinases. *J Biol Chem* **266**: 24249–24252.

Oneyama C, Hikita T, Nada S, Okada M. (2008). Functional dissection of transformation by c-Src and v-Src. *Genes Cells* **13**: 1–12.

Ong SH, Hadari YR, Gotoh N, Guy GR, Schlessinger J, Lax I. (2001). Stimulation of phosphatidylinositol 3-kinase by fibroblast growth factor receptors is mediated by coordinated recruitment of multiple docking proteins. *Proc Natl Acad Sci USA* **98**: 6074–6079.

Penuel E, Martin G. (1999). Transformation by v-Src: Ras-MAPK and PI3K-mTOR mediate parallel pathways. *Mol Biol Cell* **10**: 1693–1703.

Petroulakis E, Mamane Y, Le Bacquer O, Shahbazian D, Sonenberg N. (2006). mTOR signaling: implications for cancer and anticancer therapy. *Br J Cancer* **94**: 195–199.

Sabatini DM. (2006). mTOR and cancer: insights into a complex relationship. *Nat Rev Cancer* **6**: 729–734.

Shenouda SK, Alahari SK. (2009). MicroRNA function in cancer: oncogene or a tumor suppressor? *Cancer Metast Rev* **28**: 369–378.

Trudel S, Ely S, Farooqi Y, Affer M, Robbiani DF, Chesi M *et al.* (2004). Inhibition of fibroblast growth factor receptor 3 induces differentiation and apoptosis in t(4;14) myeloma. *Blood* **103**: 3521–3528.

van Rhijn BW, Lurkin I, Radvanyi F, Kirkels WJ, van der Kwast TH, Zwarthoff EC. (2001). The fibroblast growth factor receptor 3 (FGFR3) mutation is a strong indicator of superficial bladder cancer with low recurrence rate. *Cancer Res* **61**: 1265–1268.

Ventura A, Jacks T. (2009). MicroRNAs and cancer: short RNAs go a long way. *Cell* **136**: 586–591.

Vojtechova M, Tureckova J, Kucerova D, Sloncova E, Vachtenheim J, Tuhackova Z. (2008). Regulation of mTORC1 signaling by Src kinase activity is Akt1-independent in RSV-transformed cells. *Neoplasia* **10**: 99–107.

Wang FZ, Weber F, Croce C, Liu CG, Liao X, Pellett PE. (2008). Human cytomegalovirus infection alters the expression of cellular microRNA species that affect its replication. *J Virol* **82**: 9065–9074.

Wong TS, Liu XB, Wong BY, Ng RW, Yuen AP, Wei WI. (2008). Mature miR-184 as potential oncogenic microRNA of squamous cell carcinoma of tongue. *Clin Cancer Res* **14**: 2588–2592.

Wullschleger S, Loewith R, Hall MN. (2006). TOR signaling in growth and metabolism. *Cell* **124**: 471–484.

Yamada H, Yanagisawa K, Tokumaru S, Taguchi A, Nimura Y, Osada H *et al.* (2008). Detailed characterization of a homozygously deleted region corresponding to a candidate tumor suppressor locus at 21q11–21 in human lung cancer. *Genes Chromosomes Cancer* **47**: 810–818.

Yeatman TJ. (2004). A renaissance for SRC. *Nat Rev Cancer* **4**: 470–480.

Yokota J, Kohno T. (2004). Molecular footprints of human lung cancer progression. *Cancer Sci* **95**: 197–204.

Supplementary Information accompanies the paper on the Oncogene website (http://www.nature.com/onc)

ANTICANCER RESEARCH *31*: 4665-4672 (2011)

Low Dihydropyrimidine Dehydrogenase Correlates with Prolonged Survival in Patients with Lung Adenocarcinoma Treated with 5-Fluorouracil

YASUSHI SHINTANI[1], MASAYOSHI INOUE[1], YASUNOBU FUNAKOSHI[2], AKIHIDE MATSUMURA[3], MITSUNORI OHTA[4], HAJIME MAEDA[2] and MEINOSHIN OKUMURA[1]

[1]*Department of Thoracic Surgery, Osaka University Graduate School of Medicine, Osaka, Japan;*
[2]*Department of General Thoracic Surgery, National Hospital Organization Toneyama Hospital, Osaka, Japan;*
[3]*Department of General Thoracic Surgery, National Hospital Organization Kinki Chuo Chest Medical Center, Osaka, Japan;*
[4]*Department of General Thoracic Surgery, Osaka Prefectural Medical Center for Respiratory and Allergic Disease, Osaka, Japan*

Abstract. *Background: The enzyme dihydropyrimidine dehydrogenase (DPD) is involved in the metabolism of 5-fluorouracil (5-FU). The aim of this study was to clarify the correlation between the expression of DPD and the efficacy of 5-FU therapy in patients with lung adenocarcinoma (AD). Patients and Methods: We examined surgically resected specimens from 90 stage I to IIIA patients with lung ADs to determine the level of intra-tumoral DPD mRNA. Results: Administration of 5-FU improved the prognosis of patients with low DPD-expressing tumors, whereas it did not do so for patients with high DPD expressing tumors. Patients with low DPD-expressing tumors administered with 5-FU had a significantly better prognosis than those who underwent surgery alone. A Cox proportional hazards regression model revealed that administration of 5-FU was an independent variable to predict prognosis in patients with low DPD-expressing tumors. Conclusion: Quantification of DPD mRNA levels is useful for determining the subgroup of lung AD patients who would benefit most from 5-FU after surgery.*

5-Fluorouracil (5-FU) and its derivatives are widely used for treatment of various types of cancer (1). A recent study showed that postoperative oral administration of tegafur-uracil (UFT) improves survival in patients following resection of stage I lung adenocarcinoma (AD) and its administration has become standard therapy after curative resection in early non-small cell lung cancer (NSCLC) cases (2, 3). Furthermore, a novel oral form of fluorouracil S-1 was shown to have promising effects against advanced NSCLC (4). These findings indicate that 5-FU is effective for NSCLC patients and highlight the importance of detection of biomarkers for prediction of its efficacy for treating NSCLC.

Thymidylate synthase (TYMS), the target enzyme for 5-FU, catalyzes an important process for DNA biosynthesis (5, 6) and we previously reported that the prognosis of NSCLC patients is related significantly to the intratumoral *TYMS* mRNA level (7). Dihydropyrimidine dehydrogenase (DPD) is one of the key enzymes involved in the catabolism of 5-FU and its expression was found useful in predicting the efficacy of 5-FU after surgery for NSCLC based on disease-free interval during short follow-up periods (8-10). In the present study, we examined the efficacy of 5-FU in association with DPD expression in regards to prognosis, including overall survival, in patients with lung ADs over a longer follow-up period.

Patients and Methods

Ninety specimens from lung AD patients determined to be p-stage I to IIIA were obtained during surgical procedures at Osaka University Hospital, Kinki Chuo Chest Medical Center, Toneyama Hospital, and Osaka Prefectural Medical Center for Respiratory and Allergic Disease between January 1999 and March 2003. Quantification of *TYMS* and *DPD* mRNA levels in AD tissues was performed as described previously (7, 10). The obtained copy numbers of *TYMS* and *DPD* were standardized with glyceralde-hydo-3-phosphate dehydrogenase (*GAPDH*) mRNA quantity, used as an endogenous control, with the following equation: 'Result'=Log (*TYMS* or *DPD* RNA copy number in tumor)/(*GAPDH* RNA copy number in tumor)×(6.1×10^9; *GAPDH* RNA copy number in 1 μg of total RNA extracted from the peripheral blood of 30 healthy volunteers).

Correspondence to: Yasushi Shintani, MD, Ph.D., Department of General Thoracic Surgery, Osaka University Graduate School of Medicine, 2-2-L5, Yamadaoka, Suita-city, Osaka, 565-0871, Japan. Tel: +81 668793152, Fax: +81 668793164, e-mail: yshintani@thoracic.med.osaka-u.ac.jp

Key Words: Lung adenocarcinoma, 5-fluorouracil, dihydropyrimidine dehydrogenase, thymidylate synthase, chemosensitivity.

0250-7005/2011 $2.00+.40

Table I. *Patient background data.*

Variable	Treatment		
	Surgery alone (control) n=60	5-FU n=30	*p*-Value
Age (years)	63±9.3	62±9.4	0.445
Gender			
Male	35 (58%)	20 (67%)	0.426
Female	25 (42%)	10 (33%)	
Pathologic stage			
I	38 (63%)	20 (67%)	
II	9 (15%)	6 (20%)	0.882
IIIA	13 (22%)	4 (13%)	

5-FU, 5-fluorouracil. *p*-Value, chi-square test or Mann-Whitney *U*-test.

Table II. *Thymidylate synthase (TYMS) and Dihydropyrimidine dehydrogenase (DPD) mRNA levels, and clinicopathologic factors.*

Factor	n	Log TYMS mRNA	*p*-Value	Log DPD mRNA	*p*-Value
Tumor status			0.029		0.054
pT1	49	6.90±0.29		6.89±0.48	
pT2	36	7.03±0.33		6.63±0.54	
pT3	5	7.42±0.54		6.99±0.27	
Nodal status			0.600		0.546
pN0	61	6.96±0.34		6.80±0.57	
pN1	12	7.00±0.36		6.75±0.41	
pN2	17	7.04±0.35		6.80±0.33	

p-Value, chi-square test or Mann-Whitney *U*-test.

Informed consent was obtained from all patients. Those administered UFT following surgery comprised the 5-FU group (n=30), while those who underwent surgery only, comprised the control group (n=60). UFT administration was started within 2 months after surgery and continued for more than 12 months. The dose of UFT was 300-400 mg/day and the mean duration of treatment was 21.5±7.3 months (mean±SD; range 12-26 months). The clinical backgrounds of the patients are summarized in Table I. There was no difference in clinical factors between the groups. The median follow-up period was 78±23 months (range 17-115 months) after surgery.

Chi-square, Mann-Whitney *U*, and Kruskal-Wallis tests were used to compare the results, while survival rates were estimated by the method of Kaplan and Meier and compared using log-rank test, using Statview version 5.0 for Windows (Abacus Concepts, Berkeley, CA, USA). A *p*-value of <0.05 was considered to be statistically significant.

Results

Quantification of *TYMS* and *DPD* mRNA levels in NSCLC tissues was successfully performed for all specimens. Intratumoral *TYMS* and *DPD* mRNA levels ranged from 6.28 to 8.04 (mean±SD; 6.98±0.34) and 5.36 to 8.28 (6.79±0.59), respectively. The results for *TYMS* and *DPD* mRNA levels are summarized in Table II. *TYMS* mRNA levels were associated with tumor status, while *DPD* mRNA levels were not associated with tumor or nodal status.

Thirty-five (39%) of the 90 patients developed distant metastasis after surgery. In regards to tumor stage, 12 (21%) out of 58 patients in stage I, 8 (53%) out of 15 patients in stage II, and 15 (88%) out of 17 patients in stage IIIA suffered from recurrent disease. Categorized by group, 27 (45%) out of 60 patients and 8 (27%) out of 30 in the control and 5-FU groups, respectively, had recurrence. There was no significant difference in overall survival rate between the groups (Figure 1A). Similar to a previous report (7), *TYMS* mRNA levels were significantly correlated to overall survival when dichotomized at the mean *TYMS* mRNA level (Figure 1B).

Next, we evaluated the correlation between *DPD* expression and efficacy of 5-FU. *DPD* mRNA levels were significantly correlated to overall survival in the 5-FU group, but not in the control group when dichotomized at the mean *DPD* mRNA level (Figure 2). In the 5-FU-group, the 5-year survival rate was 92% for the low DPD-expressing subgroup and 68% for the high DPD-expressing subgroup. Patients with low DPD-expressing tumors, who were administered 5-FU had a significantly better prognosis than those who underwent surgery alone (Figure 3A); the 5-year survival rates were 92% for the 5-FU group and 53% for the control group. These findings suggest that the intratumoral *DPD* mRNA level may be a possible predictor for efficacy of 5-FU administration after surgery for NSCLC. On the other hand, patients with high DPD-expressing tumors administered 5-FU had a tendency for a worse prognosis as compared to those who underwent surgery alone (Figure 3B).

We analyzed 5 variables, namely tumor status, nodal metastasis, *TYMS* mRNA expression, *DPD* mRNA expression, and 5-FU administration, using a Cox proportional hazards regression model to determine their effects on overall survival in NSCLC patients (Table IIIA). Multivariate analysis revealed that p-N2 and *TYMS* mRNA expression were independent variables for predicting overall survival (Table IIIB). Furthermore, in patients with low DPD-expressing tumors, multivariate analysis showed that *TYMS* mRNA expression and administration of 5-FU, were each independent variables predicting prognosis (Table IIIC).

Discussion

We performed quantitative assays of intratumoral *TYMS* and *DPD* mRNA levels to assess their association with clinicopathological factors, as well as the feasibility of applying them to predict the efficacy of 5-FU therapy in

patients with NSCLC over a long term. TYMS activity is necessary for cell proliferation because it catalyses an essential step in DNA synthesis, while its overexpression is reported to be associated with tumor proliferation, as well as poor prognosis, in a variety of cancer types (11, 12). As shown in Table IIIB, multivariate analysis revealed that a high level of *TYMS* mRNA was independently correlated to overall survival with a high hazard ratio, indicating that this marker can precisely perform prognosis for patients with lung AD. Determination of gene expression by RT-PCR is a useful technique for small-sized specimens, thus quantification of *TYMS* mRNA levels is clinically sensitive and useful for determining the prognosis of AD patients (7).

As DPD is a rate-limiting enzyme in the catabolism of 5-FU, its high expression in tumors is reported to result in a low sensitivity to 5-FU therapy (13). In the present study, we evaluated the efficacy of 5-FU administration as adjuvant chemotherapy, in relation to intratumoral *DPD* mRNA levels in lung AD patients. Our results revealed that *DPD* expression was significantly inversely correlated to the overall survival of patients administered 5-FU following surgery, indicating that patients with low levels of *DPD* expression in cancer tissue are sensitive to 5-FU. Furthermore, for patients with low DPD-expressing tumors, those administered 5-FU had a significantly better prognosis than those who underwent surgery alone. These findings suggest that the intratumoral *DPD* mRNA level is a possible predictor for the efficacy of 5-FU administration after surgery in lung AD patients. Interestingly, in patients with high DPD-expressing tumors, those administered 5-FU had a tendency for worse prognosis than those who underwent surgery alone (Figure 3B), suggesting that 5-FU may not have benefits for patients with high DPD-expressing tumors. Multivariate analysis showed that administration of 5-FU was an independent variable predicting prognosis of patients with low DPD-expressing lung ADs. Based on these results, determination of *DPD* mRNA levels in lung AD tumors may provide important information for clinicians to decide whether or not to proceed with 5-FU-based chemotherapy for their patients.

Based on our findings for biomarkers associated with 5-FU therapy, it is considered important to evaluate the expressions of TYMS and DPD before establishing a protocol for made-to-order chemotherapy for NSCLC patients (14). In addition, investigation of the effects of more aggressive adjuvant therapy for patients with NSCLC who have elevated *TYMS* or *DPD* mRNA levels is also necessary. Takizawa *et al.* reported that *in vitro* sensitivity to platinum-derived drugs, such as cisplatin and carboplatin, was associated with the expression of *TYMS* and *DPD* in NSCLC specimens (15). They hypothesized that these may be novel markers of DNA repair capacity and may also be linked with chemosensitivity to drugs other than 5-FU. Furthermore, it is important to clarify the roles of TYMS and DPD in regards to chemosensitivity toward various chemotherapy regimens, as their inhibition is now receiving attention for new cancer treatment drugs development. Recently, S-1, a combination of tegafur, gimeracil, and oteracil potassium (Taiho Pharmaceutical), was developed for clinical use (4). Gimeracil is a stronger inhibitor of DPD than uracil when used with UFT. However, Takeda *et al.* reported that a high level of DPD expression predicted resistance to S-1-based chemotherapy in patients with advanced NSCLC (16). Therefore, additional investigations of the effects of new

Table III.

A. Univariate analysis of overall survival in all patients.

Factors	Hazard ratio	95% CI	*p*-Value
Tumor status			
pT3 *vs.* pT1	3.71	1.05-13.2	0.042
pT2 *vs.* pT1	1.91	0.93-3.90	0.079
Nodal status			
pN2 *vs.* pN0	3.33	1.54-7.21	0.002
pN1 *vs.* pN0	1.73	0.67-4.45	0.259
TYMS mRNA			
High *vs.* low	4.17	1.81-9.03	0.001
DPD mRNA			
High *vs.* low	1.09	0.55-2.520	0.804
Administration			
5-FU *vs.* none	1.46	0.68-3.15	0.337

B. Multivariate analysis of overall survival in all patients.

Factor	Hazard ratio	95% CI	*p*-Value
Tumor status			
pT3 *vs.* pT1	2.51	0.69-9.12	0.161
pT2 *vs.* pT1	1.27	0.59-2.75	0.546
Nodal status			
pN2 *vs.* pN0	2.56	1.16-5.66	0.020
pN1 *vs.* pN0	1.41	0.51-3.87	0.511
TYMS mRNA			
High *vs.* low	3.42	1.46-8.02	0.005

C. Multivariate analysis of overall survival in patients with low DPD-expressing tumors.

Factor	Hazard ratio	95% CI	*p*-Value
Nodal status			
pN2 *vs.* pN0	1.42	0.42-4.76	0.570
pN1 *vs.* pN0	0.85	0.22-3.27	0.816
TYMS mRNA			
High *vs.* low	5.31	1.17-24.0	0.030
Administration			
5-FU *vs.* none	7.60	1.02-56.7	0.050

CI, Confidence interval. TYMS, Thymidylate synthase. DPD, Dihydropyrimidine dehydrogenase. 5-FU, 5-fluorouracil.

A

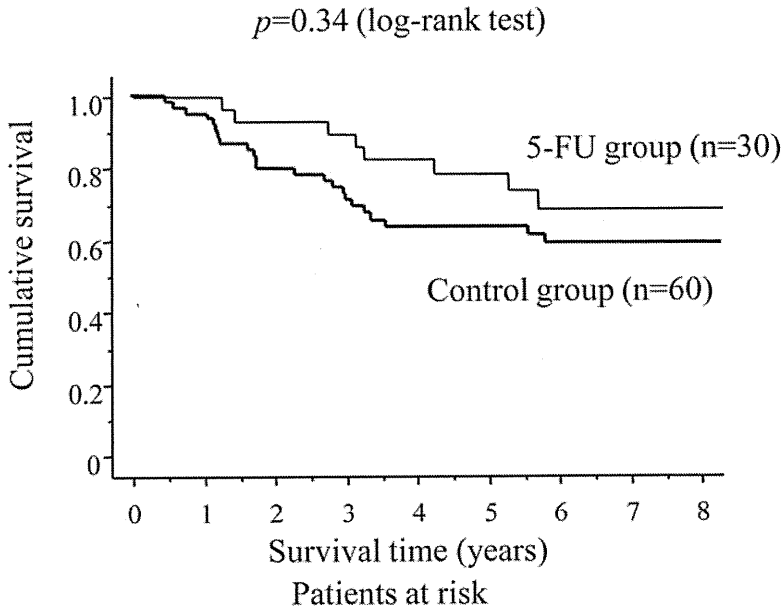

Patients at risk

Control	60	47	32	24	12
5-FU	30	27	22	12	6

B

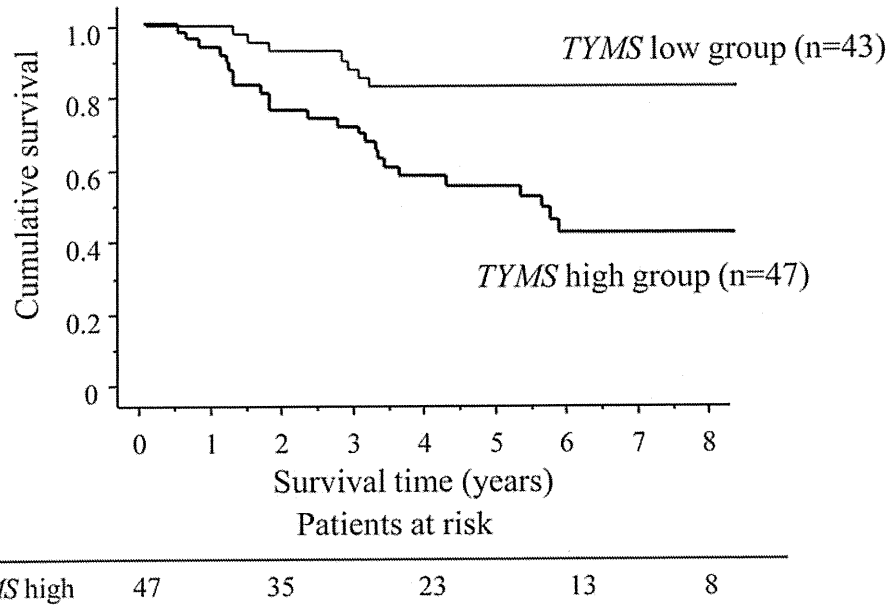

Patients at risk

TYMS high	47	35	23	13	8
TYMS low	43	39	31	23	10

Figure 1. *A: Overall survival curves for patients administered and those not administered 5-fluorouracil (5-FU) after surgery. B: Overall survival curves for patients with high and low thymidylate synthase (TYMS) mRNA levels in resected cancer tissues when dichotomized at the mean TYMS mRNA level.*

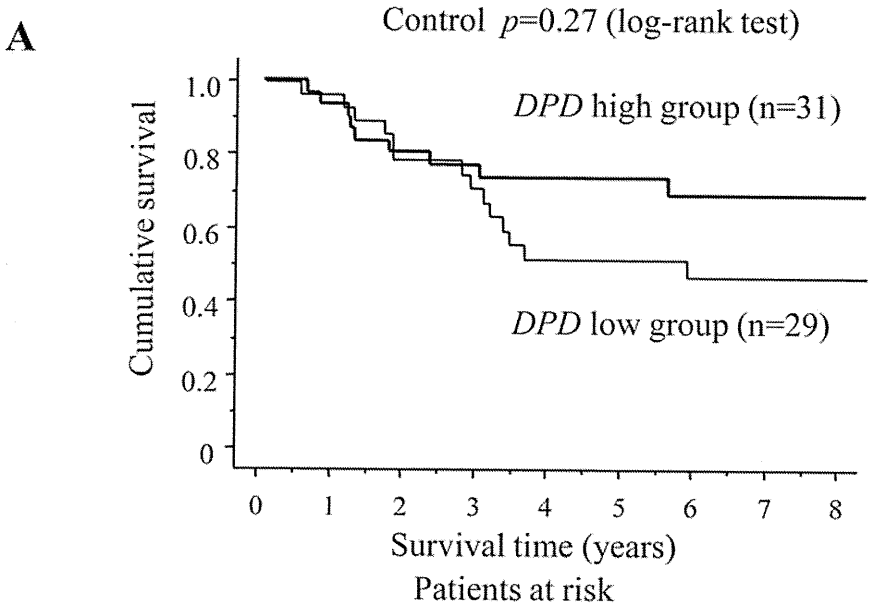

Patients at risk

DPD high	31	25	19	14	7
DPD low	29	22	13	10	5

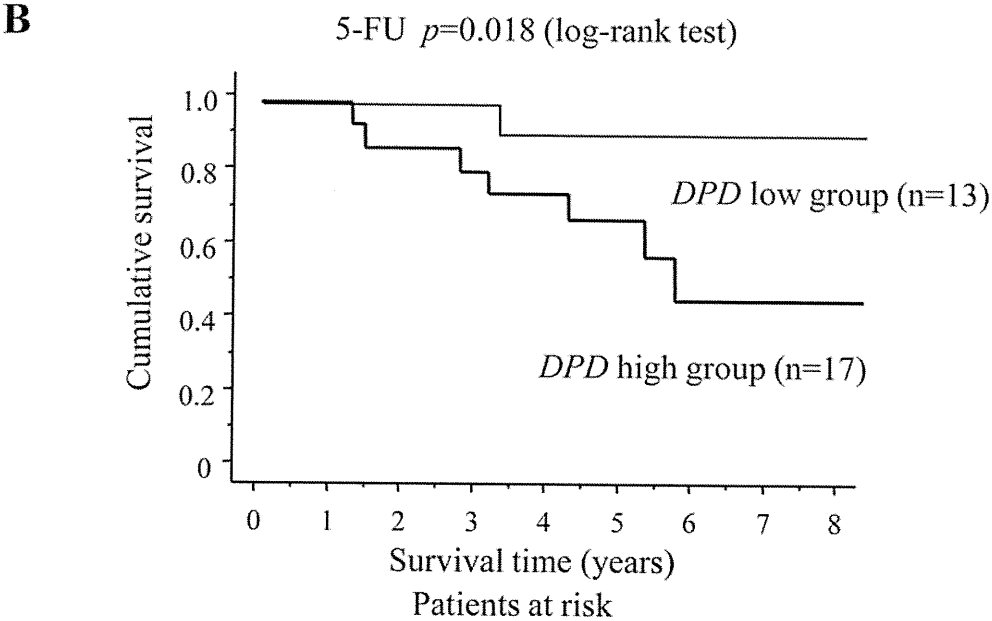

Patients at risk

DPD high	17	14	11	3	2
DPD low	13	13	11	9	4

Figure 2. *A: Overall survival curves for patients with low and high dihydropyrimidine dehydrogenase (DPD)-expressing tumors who did not receive 5-fluorouracil (5-FU) when dichotomized at the mean DPD mRNA level. B: Overall survival curves for patients with low and high DPD-expressing tumors who received 5-FU.*

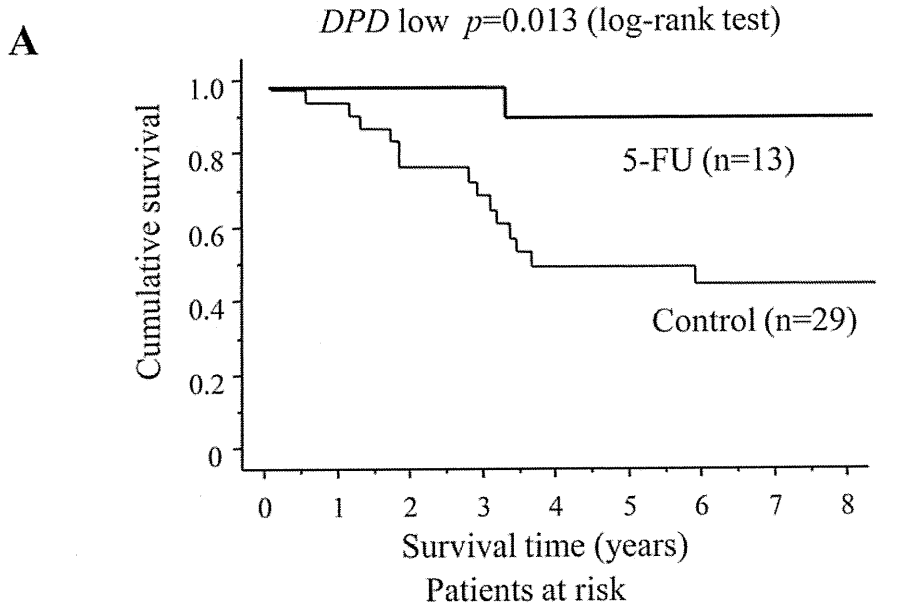

Patients at risk

Control	29	22	13	10	5
5-FU	13	13	11	9	4

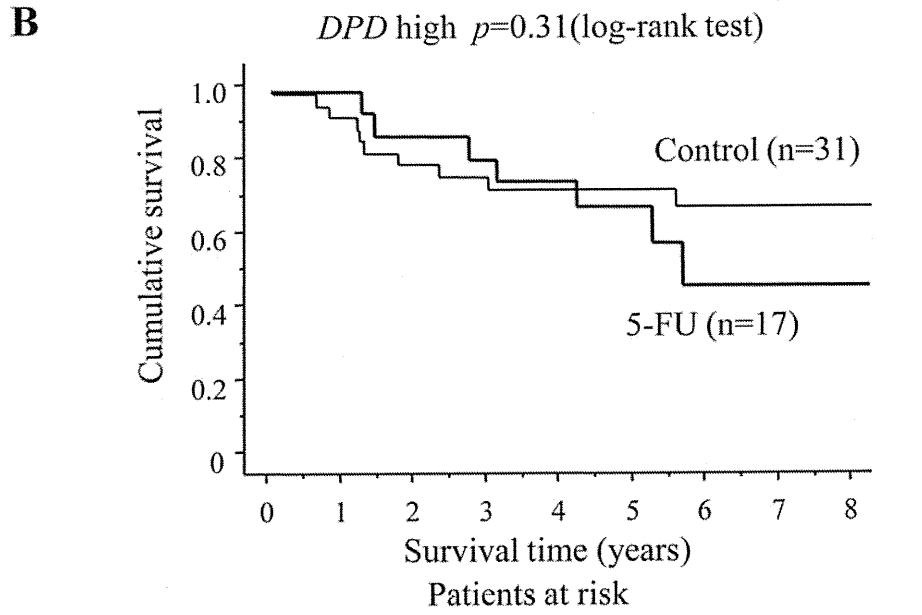

Patients at risk

Control	31	25	19	14	7
5-FU	17	14	11	3	2

Figure 3. *A: Overall survival curves for patients with dihydropyrimidine dehydrogenase (DPD)-expressing tumors: comparison between those who underwent surgery alone and those who received 5-fluorouracil (5-FU) when dichotomized at the mean TYMS mRNA level. B: Overall survival curves for patients with high DPD-expressing tumors: comparison between those who underwent surgery alone and those who received 5-FU.*

regimens with other anticancer drugs and molecular targeting therapies for NSCLC patients with high DPD-expressing tumors are necessary.

In conclusion, using real-time RT-PCR, assessment of *TYMS* and *DPD* expressions in tumors from patients with NSCLC can provide precise prognostic information and predict the efficacy of 5-FU therapy after resection.

Conflicts of Interest Statement

The Authors have no conflicts of interest to declare.

References

1 Oguri T, Achiwa H, Bessho Y, Muramatsu H, Maeda H, Niimi T, Sato S and Ueda R: The role of thymidylate synthase and dihydropyrimidine dehydrogenase in resistance to 5-fluorouracil in human lung cancer cells. Lung Cancer *49*: 345-351,2005.

2 Kato H, Ichinose Y, Ohta M, Hata E, Tsubota N, Tada H, Watanabe Y, Wada H, Tsuboi M, Hamajima N and Ohta M; Japan Lung Cancer Research Group on Postsurgical Adjuvant Chemotherapy: A randomized trial of adjuvant chemotherapy with uracil-tegafur for adenocarcinoma of the lung. N Engl J Med *350*: 1713-1721, 2004.

3 Hamada C, Tanaka F, Ohta M, Fujimura S, Kodama K, Imaizumi M and Wada H: Meta-analysis of postoperative adjuvant chemotherapy with tegafur-uracil in non-small cell lung cancer. J Clin Oncol *23*: 4999-5006, 2005.

4 Ichinose Y, Yoshimori K, Sakai H, Nakai Y, Sugiura T, Kawahara M and Niitani H: S-1 plus cisplatin combination chemotherapy in patients with advanced non-small cell lung cancer: a multi-institutional phase II trial. Clin Cancer Res *10*: 7860-7864, 2004.

5 Danenberg PV: Thymidylate synthetase: a target enzyme in cancer chemotherapy. Biochem Biophys Acta *473*: 73-92, 1977.

6 Jonston PG, Lenz HJ and Leichman CG: Thymidylate syntase gene and protein expression correlate and are associated with response to 5-fluorouracil in human colorectal and gastric tumor. Cancer Res *55*: 1407-1412, 1995.

7 Shintani Y, Ohta M, Hirabayashi H, Tanaka H, Iuchi K, Nakagawa K, Maeda H, Kido T, Miyoshi S and Matsuda H: New prognostic indicator for non-small cell lung cancer, quantitation of thymidylate synthase by real-time reverse transcription polymerase chain reaction. Int J Cancer *104*: 790-795, 2003.

8 Fischel JL, Etienne MC, Spector T, Formento P, Renee N and Milano G: Dihydropyrimidine dehydrogenase: a tumoral target for fluorouracil modulation. Clin Cancer Res *1*: 991-6, 1995.

9 Salonga D, Danenberg KD, Johnson M, Metzger R, Groshen S, Tsao-Wei DD, Lenz HJ, Leichman CG, Leichman L, Diasio RB and Danenberg PV: Colorectal tumors responding to 5-fluorouracil have low gene expression levels of dihydropyrimidine dehydrogenase, thymidylate synthase, and thymidine phosphorylase. Clin Cancer Res *6*: 1322-1327, 2000.

10 Shintani Y, Ohta M, Hirabayashi H, Tanaka H, Iuchi K, Nakagawa K, Maeda H, Kido T, Miyoshi S and Matsuda H: Thymidylate synthase and dihydropyrimidine dehydrogenase mRNA levels in tumor tissues and the efficacy of 5-fluorouracil in patients with non-small cell lung cancer. Lung Cancer *45*: 189-196, 2004.

11 Lenz HJ, Leichman CG, and Danenberg KD: Thymidylate synthase mRNA level in adenocarcinoma of the stomach: a predictor for primary tumor response and overall survival. J Clin Oncol *14*: 176-182, 1995.

12 Yamachika T, Nakanishi H, Inada K, Tsukamoto T, Kato T, Fukushima M, Inoue M and Tatematsu M: A new prognostic factor for colorectal carcinoma, thymidylate synthase, and its therapeutic significance. Cancer *82*: 70-77, 1998.

13 Harris BE, Song R, Soong SJ and Diasio RB: Relationship between dihydropyrimidine dehydrogenase activity and plasma 5-fluorouracil levels with evidence for circadian variation of enzyme activity and plasma drug levels in cancer patients receiving 5-fluorouracil by protracted continuous infusion. Cancer Res *50*: 197-201, 1990.

14 Nakano J, Huang C, Liu D, Masuya D, Nakashima T, Yokomise H, Ueno M, Wada H and Fukushima M: Evaluations of biomarkers associated with 5-FU sensitivity for non-small cell lung cancer patients postoperatively treated with UFT. Br J Cancer *95*: 607-615, 2006.

15 Takizawa M, Kawakami K, Obata T, Matsumoto I, Ohta Y, Oda M, Sasaki T and Watanabe G: *In vitro* sensitivity to platinum-derived drugs is associated with expression of thymidylate synthase and dihydropyrimidine dehydrogenase in human lung cancer. Oncol Rep 15: 1533-1539, 2006.

16 Takeda M, Okamoto I, Hirabayashi N, Kitano M and Nakagawa K: Thymidylate synthase and dihydropyrimidine dehydrogenase expression levels are associated with response to S-1 plus carboplatin in advanced non-small cell lung cancer. Lung Cancer *73*: 103-109, 2011.

Received September 13, 2011
Revised November 17, 2011
Accepted November 18, 2011

Surg Today (2012) 42:238–244
DOI 10.1007/s00595-011-0031-6

ORIGINAL ARTICLE

Clinical implications of the margin cytology findings and margin/tumor size ratio in patients who underwent pulmonary excision for peripheral non-small cell lung cancer

Noriyoshi Sawabata · Hajime Maeda · Akihide Matsumura · Mitsunori Ohta · Meinoshin Okumura · The Thoracic Surgery Study Group of Osaka University

Received: 25 October 2010 / Accepted: 1 March 2011 / Published online: 10 November 2011

Abstract
Purpose A pulmonary wedge resection is useful for the treatment of peripheral non-small cell lung cancer (NSCLC). The margin/tumor size ratio (*M/T*) is a predictor of positive margin cytology findings in these procedures, although the long-term clinical implications remain unclear. This relationship was investigated in this study.
Methods Thirty-seven cases with a high surgical risk without additional pulmonary resection were selected from those accrued in a multicenter prospective study of optimal margin distance for pulmonary excision of peripheral NSCLC and followed for more than 5 years (range 5.3–14 years).
Results Both the *M/T* and margin cytology findings were indicators of cancer recurrence and survival. All seven cases of surgical margin recurrence had a cytology-positive surgical margin. The 5-year survival rate was 54.2% ($n = 24$) for $M/T < 1$ and 84.6% for $M/T \geq 1$ ($n = 13$, $P = 0.05$), while it was 38.5% for positive margin ($n = 13$) and 79.2% for negative margin ($n = 24$) cases ($P = 0.001$). In addition, the margin cytology findings were an independent prognostic factor.
Conclusion A pulmonary wedge resection for peripheral NSCLC should result in a negative malignant margin, which might be obtained from a sufficient tumor margin ratio of $M/T \geq 1$.

N. Sawabata (✉) · H. Maeda · A. Matsumura · M. Ohta · M. Okumura
Department of General Thoracic Surgery,
Osaka University Graduate School of Medicine,
2-2 Yamadaoka, Suita, Osaka 565-0871, Japan
e-mail: sawabata@thoracic.med.osaka-u.ac.jp

Keywords Non-small cell lung cancer · Pulmonary excision · Margin cytology · Margin/tumor ratio · Prognosis

Introduction

A pulmonary lobectomy is a standard strategy to treat non-small cell lung cancer (NSCLC) [1]. In addition, a sublobar resection is applied for treatment of lung cancer patients [2], because of its ability to preserving postoperative pulmonary function [3]. However, residual cancer cells following surgery can lead to cancer relapse, thus it is very important to remove such lesions completely, leaving no residual cancer cells.

The cytology findings of specimens resected from lung cancer cases that reveal a pathologic malignant negative margin occasionally show isolated cancer cells at the surgical margin [4]. Such isolated cancer cells develop into surgical margin relapse in approximately 50% of affected cases [5, 6]. A multicenter prospective study of the end point of surgical margin cytology findings was conducted to elucidate the optimal surgical margin distance in a patient with lung cancer who underwent a wedge resection procedure. That clinical study revealed the optimal distance for a pulmonary wedge resection of peripheral lung cancer to be a distance greater than the tumor size [7]. Those findings were later referred to in a clinical phase III trial of pulmonary limited resection for peripheral small-sized lesions associated with NSCLC [8].

The recommended margin distance for a malignant-free surgical margin during NSCLC wedge resection is a distance greater than the size of the tumor [7]. However, the long-term clinical implications of this standard have not been fully reported. Therefore, the present study was

conducted to investigate this issue using specimens from NSCLC patients who underwent a pulmonary wedge resection procedure without an additional resection and who were followed for more than 5 years.

Patients and methods

The original investigation was conducted from September 1999 to September 2002, and the results were published in 2004 [6]. The study enrolled a total of 202 patients with 205 lesions after the patients provided informed consent to the study protocol. Thirty-eight of those patients underwent resection using an excision technique alone, while the remaining patients underwent a lobectomy. Complete lobectomies were not performed due to cardiopulmonary impairment in 33 patients and age (greater than 80 years

Table 1 Patients' characteristics

Age (years)	
Median	71
Minimum	50
Maximum	82
Sex	
Males	20 (54)
Females	17 (46)
Tumor size (mm)	
Median	15
Minimum	5
Maximum	35
Histology	
Adenocarcinoma	32 (86)
Squamous cell carcinoma	4 (11)
Large cell carcinoma	1 (3)
Margin distance (mm)	
Median	10
Minimum	0
Maximum	25
Tumor location	
Easy	25 (68)
Difficult	12 (32)
Lobe	
Right upper	10 (27)
Right middle	1 (3)
Right lower	7 (19)
Left upper	11 (30)
Left lower	8 (22)

The percentage is shown in parentheses

Easy, easily resectable region (apex, edge and lingual); Difficult, difficult to resect region (large ovoid surface, deep in fissure and basal)

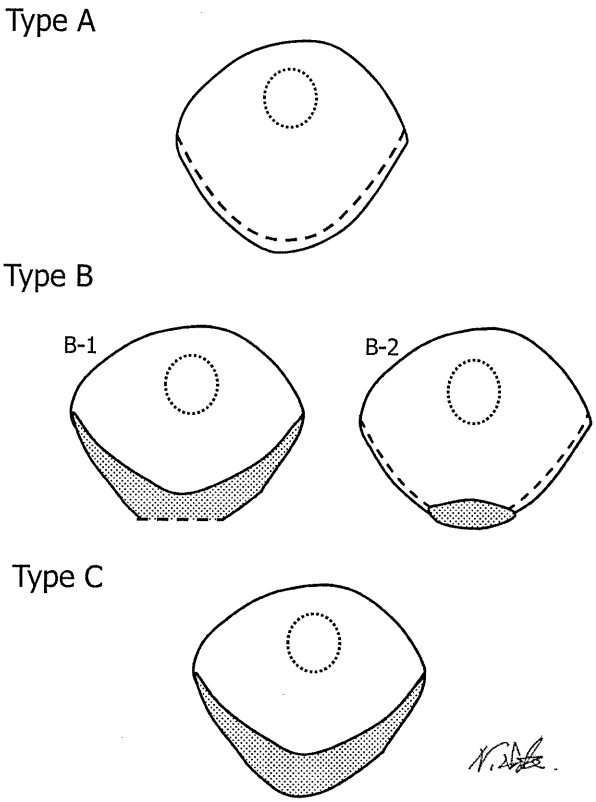

Fig. 1 Stapling methods. Type **A** entire area stapled, type *B-1* partial stapling in the proximal area, type *B-2* partial stapling in the central area, type **C** no stapling. The *broken line* illustrates staple line and the *dotted area* shows a cut surface without stapling

Table 2 Surgical results

Stapling pattern[a]	
A	24 (65)
B-1	6 (16)
B-2	1 (3)
C	6 (16)
pT	
1a	25 (67)
1b	5 (14)
2a	7 (19)
pN	
0	28 (76)
1	0 (0)
2	1 (3)
x	8 (21)
M/T	
≥1	13 (35)
<1	24 (65)
Margin cytology	
Positive	13 (35)
Negative	24 (65)

Percentages are shown in parentheses

[a] Type A, entire area stapled; type B-1, partial stapling in the proximal area; type B-2, partial stapling in the central area; type 3, no stapling

Table 3 Characteristics of patients with recurrence

No.	Age (years)	Sex	Comorbidity	Side	Segment	Location	HIS	pT	pN	Tumor size (mm)	Margin distance (mm)	*M/T*	Margin cytology	Relapse (postop, organ)	Treatment for relapse	Time to death (months)
1	77	M	Chronic empyema	R	S3	E	SQ	1	0	25	15	0.6	P	M (8 mo)	Pul. excision	24
2	52	F	Emphysema	R	S3	E	AD	1	x	25	17	0.7	P	Dm (12 mo, liver)	None	21
3	55	M	Emphysema	L	S1	D	AD	1	0	12	8	0.7	P	M (28 mo)	Lobectomy	72
4	74	M	CAD	L	S6	E	SQ	1	2	20	20	1.0	N	Dm (17 mo, brain)	RTx, brain	26
5	51	F	Emphysema	L	S3	E	AD	1	0	20	10	0.5	P	M (12 mo)	RTx, lung	22
6	70	M	Emphysema	R	S6	D	AD	1	0	20	1	0.1	P	M + Dm (4 mo, brain)	RTx, brain	14
7	61	M	Emphysema	R	S2	E	AD	1	0	35	10	0.3	N	L (4 mo, pleura)	CTx	15
8	76	F	HF	R	S6	D	AD	2	x	12	1	0.1	P	M + L (17 mo, lung)	None	29
9	69	M	Emphysema	R	S7	D	AD	1	0	20	0	0	P	L (14 mo, lung)	None	37
10	58	F	HF	L	S3	D	AD	1	0	20	0	0	P	M (14 mo)	RTx, lung	47
11	71	M	Emphysema	L	S9	D	AD	2	0	35	5	0.1	P	M (22 mo)	RTx, lung	53
12	71	M	Emphysema	L	S2	D	AD	1	0	25	25	1.0	N	Dm (32 mo, liver)	None	36
13	73	F	CAD	L	S5	D	AD	1	x	28	21	0.8	N	Dm (12 mo, bone)	None	16

HIS histology, *M/T* ratio of margin distance/tumor size, *CAD* coronary arterial disease, *HF* heart failure, *R* right, *L* left, *E* easily resectable region (apex, edge, lingual), *D* difficult to resect region (large ovoid surface, deep in fissure, basal), *SQ* squamous cell carcinoma, *AD* adenocarcinoma, *LA* large cell carcinoma, *P* positive, *N* negative, *M* margin recurrence, *L* local recurrence, *Dm* distant metastasis, *Pul* pulmonary, *RTx* radiation therapy, *CTx* chemotherapy, *mo* months

old) in 5, including 1 patient with 2 lesions who underwent an additional excision procedure; therefore, 37 patients could not undergo further proximal resection because of anatomical difficulties. Seventeen of those 37 patients were diagnosed as having NSCLC before surgery and therefore were analyzed in the present study (Table 1). Tumor location in the excision cases was classified using a method presented by Lewis et al. [9] as located in a region difficult to resect (large ovoid surface, deep in fissure, basal) or in a region easy to resect (apex, edge, lingual). The tumor size and minimum distance from the surgical margin to the tumor were measured during the procedure using the method of Sawabata et al. [5, 7, 10]. In brief, the distance from the tumor to the margin was determined using a cross section of the lesion, without removing the staples. The pattern of stapling was classified into three types (Fig. 1): totally stapled (type A), partially stapled (type B-1: central stapling, type B-2: side stapling), and totally unstapled (type C) [4]. The cells were extracted from the margin by running a glass slide was across the surgical margin to extract cells, and the cells on the side of the slide were spread onto another glass slide. Those samples were stained and examined (run-across method). The cytological examinations were carried out as quickly as possible and required approximately 10 min in each case.

The survival period was defined as the time between the dates of surgery and latest follow-up examination. The survival curves were estimated according to the Kaplan–Meier method for subsets, including the results of margin cytology and status of the margin/tumor ratio. Differences between the survival rates were evaluated using the log-rank method. Hazard ratios were calculated using a Cox regression model with age, gender, pT, pN, tumor location, stapling pattern, margin distance/tumor size ratio, and results of margin cytology used as variables. In addition, a multivariate analysis was performed using the variables that were statistically significant according to the independent Cox regression analysis. A P value of less than 0.05 was considered to be statistically significant.

Results

The surgical results are shown in Table 2, which reveals that 13 excised lungs had a margin distance/tumor ratio (M/T) ≥ 1 and 13 had malignant margin cytology findings. In addition, there were 13 cases of relapse (Table 3), including exclusive margin recurrence in 5, margin recurrence plus local recurrence in 1, margin recurrence and distant metastasis in 1, exclusive local recurrence in 2, and exclusive distant metastasis in 4. All instances of local-margin recurrence occurred in cases of lung excision with an $M/T < 1$ or with malignant margin cytology findings. The correlations among tumor size, margin distance, margin cytology, and recurrence pattern are presented in Fig. 2. There were 14 deaths during the follow-up period: 13 due to lung cancer and 1 to a cardiac event.

Disease-free survival and overall survival curves are shown in Fig. 3. The 5-year recurrence-free survival rate according to M/T was 52.3% ($n = 24$) for cases with an $M/T < 1$ and 84.6% for those with an $M/T \geq 1$ ($n = 13$, $P = 0.05$), while 30.8% of the cases showed a positive margin cytology ($n = 13$) and 82.6% were negative ($n = 24$, $P = 0.001$). The 5-year survival rate was 54.2% ($n = 24$) for cases with an $M/T < 1$ and 84.6% for those with an $M/T \geq 1$ ($n = 13$, $P = 0.05$), while 38.5% of the cases showed a positive margin cytology ($n = 13$) and 79.2% were negative ($n = 24$, $P = 0.01$). The Cox analysis findings for overall survival are shown in Table 4, which revealed that tumor location and margin cytology results were statistically significant factors. The multivariate analysis showed the margin cytology to be an independent factor (Table 5).

Discussion

The ratio of the surgical margin recurrence in patients who underwent pulmonary excision for NSCLC is approximately 50% in cases that have malignant positive margin cytology findings [5, 6, 11]. These results indicate that such a finding is a significant prognostic factor, which was confirmed in the present investigation of patients over a long-term follow-up period of greater than 5 years.

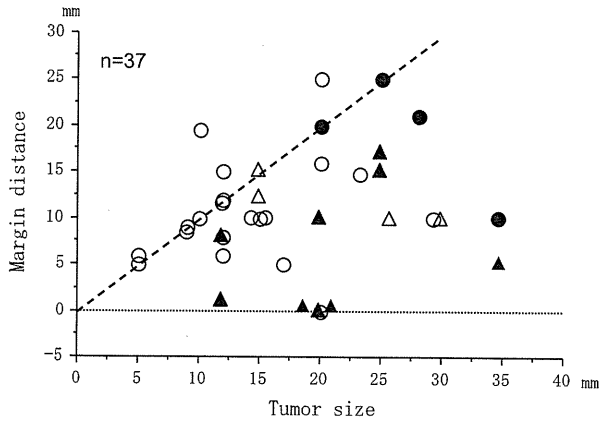

Fig. 2 Status of recurrence based on the tumor size, margin distance, and margin cytology. *Circles* show negative cytology ($n = 24$) and *triangles* positive cytology ($n = 13$) findings. *Closed circles* and *closed triangles* represent recurrence ($n = 13$). Five cases had exclusive margin recurrence, 1 had margin recurrence plus local recurrence, 1 had margin recurrence and distant metastasis, 2 had exclusive local recurrence, and 4 had exclusive distant metastasis